Autoreduction of Ferryl Myoglobin: Discrimination among the Three Tyrosine and Two Tryptophan Residues as Electron Donors†

Olivier M. Lardinois and Paul R. Ortiz de Montellano*

Department of Pharmaceutical Chemistry, University of California, 600 16th Street, San Francisco, California 94143-2280

Received December 13, 2003; Revised Manuscript Received February 15, 2004

ABSTRACT: Ferric myoglobin undergoes a two-electron oxidation in its reaction with H_2O_2. One oxidation equivalent is used to oxidize Fe(III) to the Fe(IV) ferryl species, while the second is associated with a protein radical but is rapidly dissipated. The ferryl species is then slowly reduced back to the ferric state by unknown mechanisms. To clarify this process, the formation and stability of the ferryl forms of the Tyr → Phe and Trp → Phe mutants of recombinant sperm whale myoglobin (SwMb) were investigated. Kinetic studies showed that all the mutants react normally with H_2O_2 to give the ferryl species. However, the rapid phase of ferryl autoreduction typical of wild-type SwMb was absent in the triple Tyr → Phe mutant and considerably reduced in the Y103F and Y151F mutants, strongly implicating these two residues as intramolecular electron donors. Replacement of Tyr146, Trp7, or Trp14 did not significantly alter the autoreduction, indicating that these residues do not contribute to ferryl reduction despite the fact that Tyr146 is closer to the iron than Tyr151 or Tyr103. Furthermore, analysis of the fast phase of autoreduction in the dimer versus recovered monomer of the Tyr → Phe mutant K102Q/Y103F/Y146F indicates that the Tyr151−Tyr151 cross-link is a particularly effective electron donor. The presence of an additional, slow phase of reduction in the triple Tyr → Phe mutant indicates that alternative but normally minor electron-transfer pathways exist in SwMb. These results demonstrate that internal electron transfer is governed as much by the tyrosine pK_a and oxidation potential as by its distance from the electron accepting iron atom.

Myoglobin reacts with H_2O_2 and other peroxides to give a spectroscopically detectable ferryl ($Fe^{IV}=O$) species and a transient protein radical (*1*, *2*). The protein radical can be directly observed by EPR (*1*−*4*), can be spin-trapped (*5*−*7*), and in the case of sperm whale myoglobin (SwMb),[1] gives rise to dityrosine and isodityrosine cross-linked oligomers (*8*−*10*). SwMb differs from equine and many other myoglobins in that it has three tyrosine residues (Tyr103, Tyr146, and Tyr151), whereas the equine homologue has only two (Tyr103 and Tyr146) (*11*). Analysis of the Tyr−Tyr bonds between the units in the SwMb oligomers generated by reaction with H_2O_2, in conjunction with studies of site-specific mutants in which the individual tyrosine residues were removed, confirm that Tyr151 is absolutely required for the formation of intermolecular protein cross-links (*8*, *9*, *12*). The isolation of a Tyr151−Tyr103 cross-linked species indicates that Tyr103 also bears unpaired electron density, but its self-dimerization must be sterically restricted, as it only detectably formed a dimer with Tyr151 (*12*). This readily explains the absence of oligomeric products in incubations of equine Mb with H_2O_2, as this protein lacks Tyr151. Tyr146 apparently either does not bear unpaired electron density or is not sterically available for dimerization reactions.

In addition to the two tyrosines, evidence exists for oxidation of at least one of the two tryptophan residues, Trp7 and Trp14 (*13*, *14*). The involvement of Trp14 in radical reactions is suggested by two lines of evidence: (a) the demonstration that cooxidation reactions depend on the presence of this residue, implying that oxygen binds to a Trp14 radical (*9*) and (b) spin-trapping studies in conjunction with site-specific mutagenesis and detailed EPR characterization of the trapped radical (*13*, *14*). A claim that Trp14 was not oxidized to the radical species (*15*) has been shown to reflect a peroxide-concentration dependence of the reaction (*14*), with the Trp radical being detectably spin trapped at low H_2O_2/protein ratios but only the tyrosines at higher ratios. In addition to the evidence for tyrosine and tryptophan radicals in H_2O_2-oxidized myoglobin, there is mass spectrometric evidence that other sites may make minor contributions to the radical pool formed in the protein upon oxidation (*16*).

The protein radical that is initially formed in the reaction of Mb with H_2O_2 is quenched rapidly by unknown mechanisms (*3*, *17*), leaving a small residual radical signal and the relatively long-lived ferryl species that is slowly autoreduced back to the ferric state. This autoreduction phase has not been studied in any detail and the origin of the electrons required for the autoreduction is not known, even though this reaction potentially provides a rare experimental system in which the identities and distances between the electron

† This work was supported by NIH Grant GM32488.

* To whom correspondence should be addressed. Tel: (415) 476-2903. Fax: (415) 502-4728. E-mail: ortiz@cgl.ucsf.edu.

[1] Abbreviations: Mb, myoglobin; MetMb, metmyoglobin; SwMb, sperm whale myoglobin; WT_{nat}, commercial preparation of metMb; WT_{rec}, wild-type recombinant metMb; triple Tyr → Phe mutant, K102Q/Y103F/Y146F/Y151F recombinant metMb; heme, iron protoporphyrin IX regardless of the oxidation and ligation states; EPR, electron paramagnetic resonance.

10.1021/bi036241b CCC: $27.50
Published on Web 03/25/2004

donor and electron acceptor can be defined with some precision. We report here a study of the roles of the five oxidizable aromatic residues, three tyrosines and two tryptophans, in autoreduction of the ferryl species which shows that tyrosines, but not tryptophans, contribute to the process and which reveals that the pK_a and redox potential of the tyrosine is at least as important as its distance from the acceptor site for electron transfer to occur.

EXPERIMENTAL PROCEDURES

Materials. SwMb type II acquired from Sigma was used without further purification (this product is no longer commercially available). All aqueous solutions were prepared using water passed through a Milli Q system (Millipore) equipped with a 0.2 μm pore size final filter. Diluted H_2O_2 solutions, obtained from a 30% solution (Sigma), were used within 1 h of their preparation. The H_2O_2 concentrations were confirmed from absorbance measurements at 240 nm ($\epsilon_{H_2O_2,240} = 39.4\ M^{-1}\ cm^{-1}$) (*18*). Prepacked Sephadex G-25 (PD-10) gel-filtration cartridges were purchased from Amersham Pharmacia Biotech. All other chemicals were of analytical grade and were purchased from Sigma or Roche Molecular Biochemicals.

Analytical Methods. Absorption spectra were recorded on a Cary 1E UV−vis spectrometer (Varian, Victoria, Australia), or for rapid reactions, a HiTech SF-61 DX2 stopped-flow instrument (HiTech Ltd, Salisbury, UK) equipped with a diode array detector was used. The kinetic data for the reduction of ferrylMb at 37 °C were obtained using a Hewlett-Packard 8452A UV−vis diode array spectrometer (Palo Alto, CA), or for a slower reaction at 25 °C, a Cary 1E UV−vis spectrometer was used. Gel-filtration experiments were performed on an Amersham Pharmacia Biotech fast protein liquid chromatography system (FPLC). SDS−PAGE was done on NuPAGE bis-Tris precast gels (Invitrogen, CA).

Preparation and Expression of Site-Directed Protein Mutants. The mutant SwMb proteins were expressed, purified, and oxidized to the met form as described previously (*8*, *19*). The far ultraviolet circular dichroism spectra of wild-type and mutant Mb proteins at pH 6.8 were fully superimposable (data not shown). In all the mutants examined, the UV−vis spectra observed were nearly identical to those of the native protein, indicating that changes to the structure in the vicinity of the heme iron were minimal (data not shown). The concentrations of the commercial preparation of SwMb and of the recombinant proteins were determined from the Soret maximum at 409 nm ($\epsilon_{metMb,409} = 157\ mM^{-1}\ cm^{-1}$) (*20*).

Dependence of the Oligomerization Yield on Myoglobin Concentration. SwMb stock solutions (40−2560 μM) were prepared in 50 mM potassium phosphate buffer, pH 6.8, and incubated at 25 °C. The reaction was initiated by addition of 1 equiv of H_2O_2. The resulting solutions were incubated at 25 °C for 2 h and allowed to stand at 4 °C until subjected to FPLC on a gel-filtration column as described next.

SDS−PAGE of Protein Samples. Cross-linking experiments were similarly performed in 50 mM potassium phosphate buffer, pH 6.8, at 25 °C for 5 min. The reactions were terminated by the addition of the SDS−PAGE sample buffer. Samples were allowed to stand in SDS for 10 min and heated at 100 °C for 2 min prior to loading onto the gels, which were developed and then stained with Coomasie blue.

Separation and Quantitation of SwMb Cross-Linking Products by Gel-Filtration Chromatography. Samples were diluted to a final concentration of 40 μM in heme and subjected to FPLC on a Superdex 75 HR 10/30 column with detection at 280 nm. The column was equilibrated and run at 0.50 mL/min in 50 mM potassium phosphate buffer, pH 6.8. The yield of cross-linked protein was estimated by comparing the area of earlier eluting peaks (high molecular mass) with that of the peak area obtained for metMb before addition of H_2O_2. Control experiments (not shown) established that the total area of the peaks at 280 nm remained unaffected by the polymerization. As the extinction coefficient of the native form and the degree of polymerization of the cross-linked products were known, it was possible to determine the molar concentration of the products. The relative amounts of cross-linked products were calculated by deconvolution of the FPLC traces using the software Origin from Microcal Software, Inc. (Northampton MA). The deconvolution method relies on curve-fitting the chromatograph with *a priori* specification of the number of Gaussian peaks contained in the data.

Stopped-Flow Measurements. Kinetic determinations for the reaction of the commercial preparation of SwMb with H_2O_2 were performed with a HiTech SF-61 DX2 stopped-flow spectrophotometer. All stopped flow experiments were performed in 50 mM potassium phosphate buffer, pH 6.8. Typically, 200 time-dependent spectra (linear time-base, dead-time ~2 ms, $\lambda = 325-700$ nm, resolution 1 nm) were collected over 0.3 s at 25 °C.

Data Analysis. Kinetic parameters for the autoreduction of ferrylMb to metMb were calculated by nonlinear regression analysis (the Levenberg−Marquardt algorithm) using the software Origin from Microcal Software, Inc. (Northampton MA). Kinetic data for the reaction of metMb with H_2O_2 were processed using the single-exponential equation of the HiTech software from which first-order rate constants (k_{obs}) were obtained. Apparent rate constants (k_{cat}) were then determined by linear regression. At least four determinations of the pseudo-first-order rate constants, k_{obs}, were measured for each substrate concentration, and the mean value was used to calculate the second-order rate constants.

RESULTS

Reaction of Metmyoglobin with H_2O_2 and Formation of Ferryl Myoglobin. The reaction of the commercial preparation of SwMb (WT_{nat}) with H_2O_2 was studied with a stopped-flow spectrometer equipped with a diode array detector. As shown in Figure 1B, mixing WT_{nat} and H_2O_2 resulted in decreases in peak intensities at 409, 504, and 630 nm and concomitant increases at 421, 550, and 585 nm that are associated with the formation of ferrylMb. Comparison of the spectra recorded at different time intervals reveals well-defined isosbestic points, suggesting a direct conversion without long-lived intermediates. Kinetic analyses of the stopped flow traces showed a monophasic increase in the peak intensity at 421 nm (Figure 1A, upper panel). The increase in absorbance at 421 nm was well-fit by a single-exponential function (Figure 1A, lower panel), giving a rate constant (k_{obs}) that was independent of enzyme concentration.

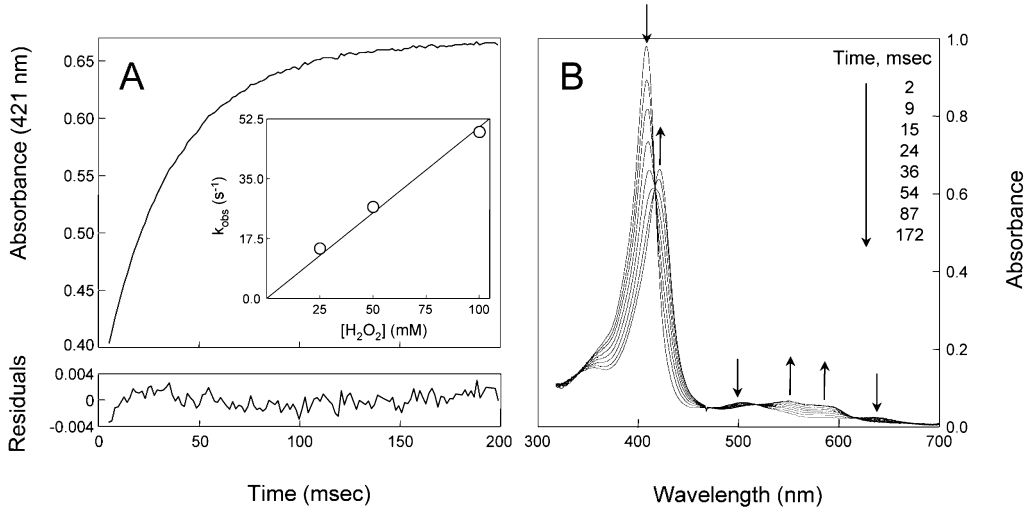

FIGURE 1: Formation of ferryl Mb from metMb and H_2O_2. (A) Top panel: time course of the reaction at 421 nm (absorption maximum of the ferryl form). Bottom panel: residuals from a nonlinear regression analysis: $A(t) = a + b \exp(-k_{obs}t)$, from which $k_{obs} = 27.71\ s^{-1}$ and $b = -0.298$, are obtained. Inset to upper panel: plot of the observed rate constants (k_{obs}) vs $[H_2O_2]$. (B) Stopped-flow rapid scan diode array spectra in the Soret and visible regions. The directions of spectral changes are indicated by arrows. Experimental conditions: commercial preparation of wild-type SwMb (6.4 μM final concentration) in 50 mM potassium phosphate buffer, pH 6.8, at 25 °C. The reaction was initiated by the addition of H_2O_2 at a final concentration of 50 mM. The measurements were performed with a stopped-flow instrument, and the data were collected using a photodiode array detector as described under Experimental Procedures.

Table 1: Apparent Rate Constants for the Reaction of the Commercial Preparation and the Recombinant Proteins with H_2O_2 Obtained using an Ordinary Dual Beam Spectrophotometer[a]

	$k_{cat} \times 10^{-2}$[b] ($M^{-1}\ s^{-1}$)
WT_{nat}	4.92 ± 0.07
WT_{rec}	4.5 ± 0.2
W7F	3.92 ± 0.05
W14F	4.25 ± 0.07
Y146F	4.88 ± 0.08
Y151F	4.42 ± 0.08
K102Q/Y103F[c]	4.4 ± 0.3
K102Q/Y103F/Y146F[c]	4.9 ± 0.2
K102Q/Y103F/Y146F/Y151F[c]	4.71 ± 0.08

[a] Determined in 50 mM potassium phosphate buffer (pH 6.8) at 25 °C. The reaction was initiated by the addition of H_2O_2. Solutions were hand mixed in the thermostated cell of the spectrophotometer. H_2O_2 concentrations from 5.2 to 20.8 μM were used. [b] Pseudo-first-order rate constants (k_{obs}) were calculated from the initial variations in absorbance at 408 nm. Values of k_{obs} had a linear dependence upon peroxide concentration. Apparent rate constants (k_{cat}) were then determined by linear regression from the slope of the regression line. [c] The Lys → Gln substitution at position 102 stabilizes proteins with the Tyr 103 mutation (*8*).

k_{obs} values exhibited a linear dependence on the peroxide concentration (Figure 1A, inset). An apparent rate constant (k_{cat}) of $5.0 \pm 0.2 \times 10^2\ M^{-1}\ s^{-1}$ for the reaction of WT_{nat} with H_2O_2 was determined from the slope of the line.

The data presented in Table 1 summarize the k_{cat} values for the reaction of the parent and the various recombinant proteins with H_2O_2. The rate constants presented in the table were estimated from the initial variations in absorbance at 408 nm using an ordinary dual beam spectrophotometer. H_2O_2 concentrations from 5.2 to 20.8 μM were used. The value of k_{cat} for the reaction of WT_{nat} with H_2O_2 reported in Table 1 is similar to that obtained with the stopped-flow instrument, thereby validating the experimental approach utilized. Kinetic constants for the reactions of the MetMb mutants with H_2O_2 were similar to those for the native enzyme purified from sperm whale; the rate constants for the WT_{rec} and mutant proteins differed from that of native SwMb by no more than 20% (Table 1). Tyr → Phe substitution at position 103 had no significant effect on this reaction. This is in accordance with the behavior exhibited by human Mb, for which a Y103F mutation marginally decreased the rate constant for this reaction (1.4-fold) (*21*). It was found previously that the point mutation Y103F encodes a protein that is not soluble and remains with the cell debris when the cells are lysed (*8*). For this type of Mb, the destabilizing influence of the Y103F substitution can be offset by the introduction of a second point mutation, K102Q (*8*).

Autoreduction of Ferryl Myoglobin to Metmyoglobin. Figure 2A shows the absorption changes in the Soret and visible regions during the autoreduction of ferryl Mb to metMb. H_2O_2 was added to the wild-type recombinant protein. After 10 s, the excess of H_2O_2 was removed by adding catalase. The spectrum at 0.2 min (λ_{max} 421, 547, and 575 nm) is that of the resulting ferryl Mb. On standing, the ferryl Mb was slowly converted back to metMb (λ_{max} 408, 504, and 630 nm). The time course of the autoreduction at 421 nm, the absorption maximum of the ferryl form, is complex, and at least two exponentials are required to adequately fit the absorbance changes (Figure 3A, lower panels). The fast exponential phase of the reduction is complete within minutes ($k_{1obs} = 5.24 \times 10^{-3}\ s^{-1}$, $t_{1/2} = 2.2$ min), while the subsequent slow phase occurs on a time scale of minutes to hours ($k_{2obs} = 5.73 \times 10^{-4}\ s^{-1}$, $t_{1/2} = 20.2$ min). The amplitude of the fast phase corresponds to reduction of 34% of the ferryl species.

Figure 2B shows the equivalent experiment conducted with the triple Tyr → Phe mutant. The spectrum at 0.2 min for the triple Tyr → Phe mutant is typical of ferrylMb and similar to that obtained for the wild-type recombinant protein (Figure 2A), but the conversion of ferrylMb back to the metMb form was considerably slowed. The time course of the autoreduction at 421 nm is presented in Figure 3B. Results obtained for the wild-type recombinant and the single Tyr → Phe mutants are presented in the same plot for comparison. Figure 4 summarizes the kinetic constants obtained from the

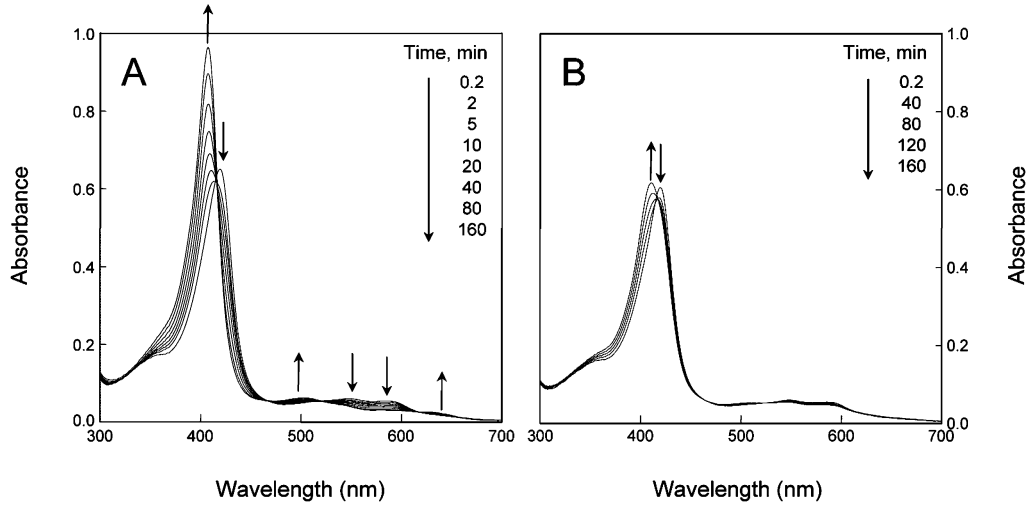

FIGURE 2: Spectral changes during the autoreduction of ferryl Mb to metMb. (A) Wild-type recombinant and (B) triple Tyr → Phe mutant. The spectral changes were measured with an ordinary dual beam spectrophotometer. Experimental conditions: SwMb (6.4 μM) in 50 mM potassium phosphate buffer, pH 6.8, at 25 °C. The reaction was initiated by the addition of H_2O_2 at a final concentration of 600 μM. After a 10 s incubation, the excess of H_2O_2 was removed by addition of catalase (26 units), and scans were taken at the time intervals indicated. A large excess of H_2O_2 was used in all the experiments to ensure complete conversion of the metMb to the ferrylform within 10 s.

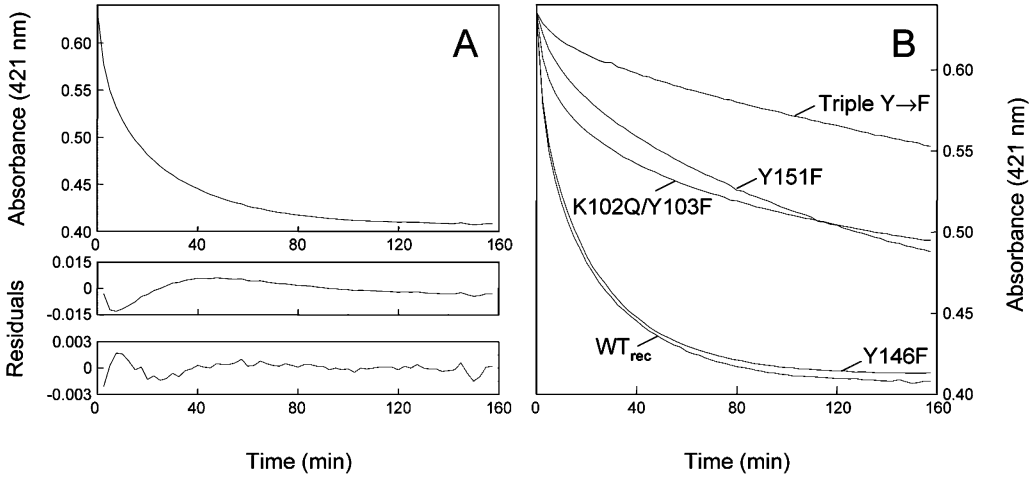

FIGURE 3: Time course of the autoreduction reaction at 421 nm (absorption maximum of the ferryl form). Incubation at 25 °C and assay conditions were as described in the legend of Figure 2. (A) Upper panel: representative trace for autoreduction of the wild-type recombinant SwMb. Middle panel: residuals from a nonlinear regression analysis: $A(t) = a + b \exp(-k_{1obs}t)$, from which $k_{1obs} = 7.96 \times 10^{-4}$ s^{-1} and $b = 0.191$, are obtained. Bottom panel: residuals from a nonlinear regression analysis: $A(t) = a + b \exp(-k_{1obs}t) + c \exp(-k_{2obs}t)$, from which $k_{1obs} = 5.24 \times 10^{-3}$ s^{-1} and $b = 0.078$ for the fast phase and $k_{2obs} = 5.73 \times 10^{-4}$ s^{-1} and $c = 0.149$ for the slow phase, are obtained. (B) Representative traces for the autoreduction of wild-type recombinant SwMb and its site-directed mutants.

spectroscopic fits at 421 nm. The kinetic traces in Figure 3B indicate that the rapid phase of the reaction is eliminated in the triple mutant, strongly implicating the tyrosines as the primary source of reducing equivalents within the enzyme. Repetition of the experiment with the single Tyr → Phe mutants showed that the rapid phase of spontaneous ferryl reduction was considerably reduced in the K102Q/Y103F and Y151F mutants (Figure 3B), strongly implicating these two tyrosine residues as sources of reducing equivalents in the enzyme. The presence of an additional slower phase still present in the triple mutant indicates that tyrosine is not the only source of reducing equivalents within the enzyme and strongly suggests that an additional but much slower electron-transfer pathway also exists. Substitutions at Tyr146, Trp7, or Trp14 have no significant effect on either the k_{1obs} or k_{2obs} values or the amplitude of the fast phase of the reaction (Figure 4). The kinetic constants obtained for all the mutants investigated in this study were independent of the enzyme concentration (not shown), implying that decay of the ferryl form occurred through an intra- rather than intermolecular electron-transfer reaction.

Protein Cross-Linking. As cross-linking could contribute to the autoreduction behavior, the extent of protein cross-links upon reaction of the recombinant enzymes with H_2O_2 was analyzed by SDS−PAGE (Figure 5). The proportions of the various reaction products were also measured by gel-filtration chromatography (Table 2). As shown in Figure 5, incubation of WT_{rec} with 1 equiv of H_2O_2 resulted in the formation of dimeric and trimeric products. Other less clear bands also appear at higher molecular weight, likely corresponding to traces of tetramers and other multimers. The relative amounts of cross-linked products formed by WT_{rec} were essentially identical to those of the native parent protein, as judged by gel-filtration chromatography (Table 2). Removal of Trp7, Trp14, Tyr103, or Tyr146 does not interfere with oligomerization of the protein. In contrast, as previously reported (*8*), the replacement of Tyr151 significantly inhibited cross-linking of the protein, and the triple tyrosine mutant

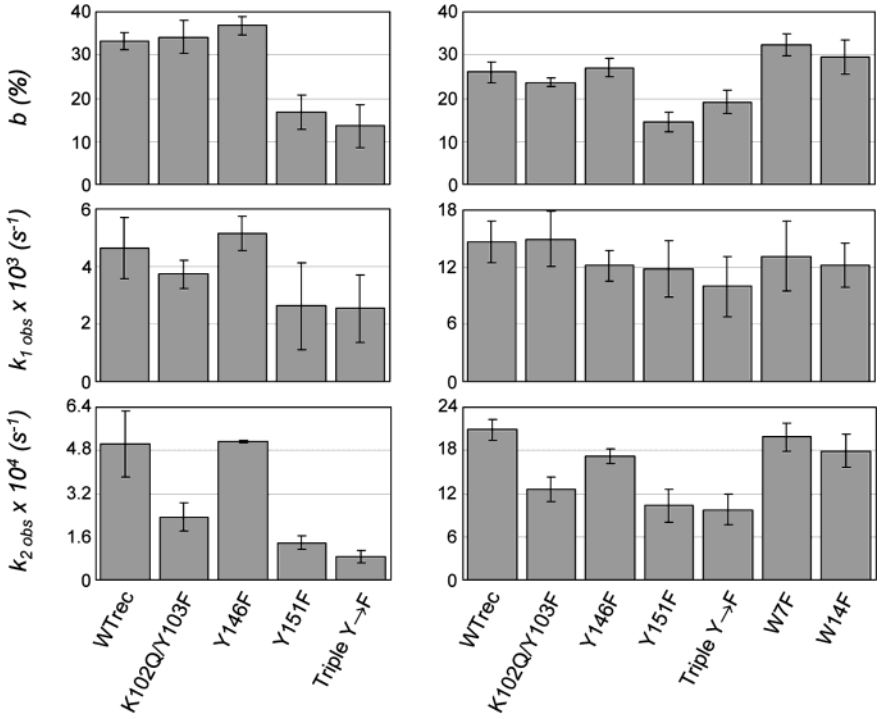

FIGURE 4: Kinetic parameters for the autoreduction of SwMb and its site-directed mutants. Left panels: incubation at 25 °C and assay conditions were as described in the legend of Figure 2. Right panels are the same as the corresponding left panels except that the experiments were conducted at 37 °C. Kinetic parameters for the fast and the slow phases of the reaction were estimated from fits of $A(t) = a + b \exp(-k_{1\,obs}t) + c \exp(-k_{2obs}t)$ to absorbance changes at 421 nm as shown in Figure 3. The upper set of results, labeled *b* (%), is the amplitude for the fast phase of the reaction normalized to the amplitude for the slow phase of the reaction (e.g., b (%) = 100 $b/(b + c)$). Values are mean ±SD ($n = 3$).

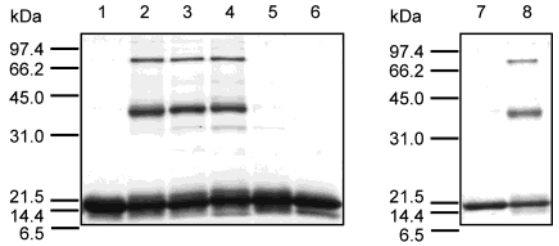

FIGURE 5: SDS-PAGE analysis of the cross-linking of SwMb and its Tyr → Phe site-directed mutants. Lane 1, WT_{rec} ; lane 2, WT_{rec} + H_2O_2; lane 3, K102Q/Y103F + H_2O_2; lane 4, Y146F + H_2O_2; lane 5, Y151F + H_2O_2; lane 6, triple Y → F mutant + H_2O_2; lane 7, K102Q/Y103F/Y146F; and lane 8, K102Q/Y103F/Y146F + H_2O_2. The following concentrations were used: [SwMb] = [H_2O_2] = 40 μM (lanes 1−6) or 20 μM (lanes 7 and 8), [polyacrylamide] = 16%. Incubations were carried out as described under Experimental Procedures and were analyzed by SDS−PAGE. The samples were reduced with 2-mercaptoethanol and were boiled before electrophoresis. The gels were overloaded with the protein samples to allow easy visualization of dimeric and trimeric products.

gave no detectable cross-linking. Interestingly, incubation of the double Tyr → Phe mutant K102Q/Y103F/Y146F with H_2O_2 resulted in the formation of dimeric and trimeric products (Figure 5, line 8 and Table 2). The formation of dimeric products, despite the absence of Tyr103 and 146, confirms that a Tyr151/Tyr151 bond is possible (*8*). The formation of trimeric products, despite the absence of Tyr103 and 146, opens up the possibility that the Tyr151 residues on the three myoglobin chains are oxidatively coupled to form trityrosine cross-links. However, attempts to identify an oxidatively coupled tyrosine trimer in hydrolysates of H_2O_2-treated K102Q/Y103F/Y146F mutant have been unsuccessful.

Table 2: Relative Amount of Cross-Linked Products Formed after Treatment of SwMb with a Stoichiometric Amount of H_2O_2[a]

	% total Mb chain[b]		
	dimer	trimer	oligomer
WT_{nat}	32.5 ± 0.2	11 ± 4	8 ± 7
WT_{rec}	28.9 ± 0.4	10 ± 3	7 ± 3
W7F	34.0 ± 0.3	10 ± 3	7 ± 3
W14F	32.7 ± 0.3	11 ± 4	6 ± 4
Y146F	28.5 ± 0.4	12 ± 3	8 ± 3
Y151F	4.3 ± 0.5	nd[c]	nd[c]
K102Q/Y103F	30.3 ± 0.3	9 ± 3	4 ± 3
K102Q/Y103F/Y146F	27.5 ± 0.6	5 ± 6	5 ± 6
K102Q/Y103F/Y146F/Y151F	nd[c]	nd[c]	nd[c]

[a] Experimental conditions: SwMb (40 μM) in 50 mM potassium phosphate buffer, pH 6.8, at 25 °C. The reaction was initiated by the addition of 1 equiv H_2O_2. The resulting solutions were incubated at 25 °C for 2 h and allowed to stand at 4 °C until subjected to FPLC as described under Experimental Procedures. [b] The relative amounts of cross-linked products formed were calculated by deconvolution of the FPLC traces at 280 nm as described under Experimental Procedures. The number of Gaussian peaks contained in each chromatograph was fixed to four. [c] Not detectable.

We next investigated the dependence of the oligomerization yields on the protein concentration when the H_2O_2/Mb ratio is held constant at 1.0. Typical elution profiles for the WT_{rec} protein are given in Figure 6A. Peak 1 migrates in the same position as the monomer. Treatment of the WT_{rec} protein with H_2O_2 leads to a decrease in peak 1 and the appearance of two well-defined higher molecular weight peaks, peak 2 (∼38 kDa) and peak 3 (∼52 kDa), which correspond to dimeric and trimeric products, respectively. At the highest concentrations of Mb, a new peak (peak 4) can be seen in the figure as a distinct shoulder on the edge of peak 3. This new peak corresponds to tetrameric products

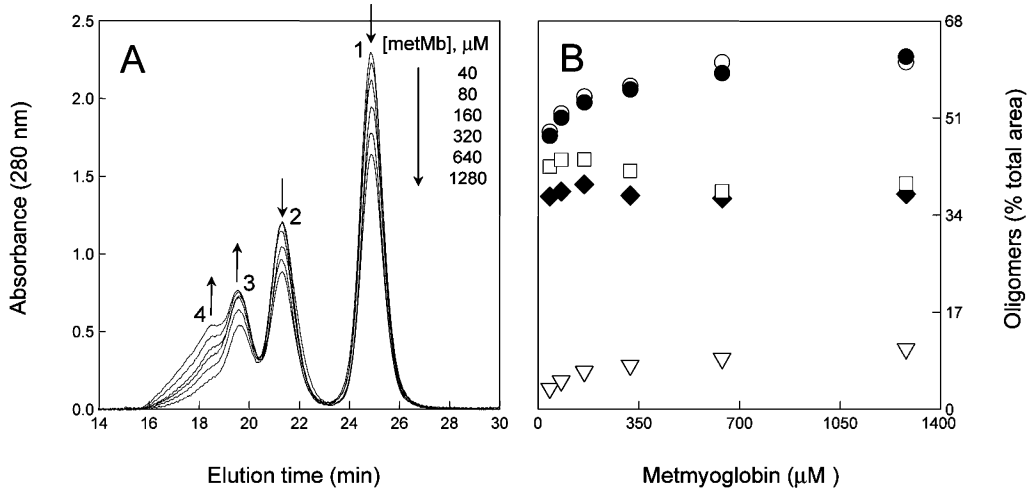

FIGURE 6: Dependence of the oligomerization reaction on the Mb concentration. (A) Variation of elution profiles on a gel-filtration column. Experimental conditions were as follows: wild-type recombinant SwMb (40−1280 μM) in 50 mM potassium phosphate buffer, pH 6.8, at 25 °C. The reaction was initiated by the addition of 1 equiv of H_2O_2. Resulting solutions were incubated at 25 °C for 2 h and stored at 4 °C before being chromatographed on a gel-filtration column. Direction of chromatographic changes is indicated by arrows. (B) Effect of increasing Mb concentration on oligomerization yields. Experiments were conducted as described in the legend of panel A. The oligomerization yields were calculated from the gel-filtration elution profiles and expressed as a percentage of the chromatographic peak area at 280 nm obtained for metMb before addition of H_2O_2. ●, WT_{rec}; ○, Y146F; ▽, Y151F; □, K102Q/Y103F; and ◆, K102Q/Y103F/Y146F.

with a molecular weight of about 72 kDa. Interestingly, and as noted in a previous investigation with the commercial native enzyme (*10*), all of the intensity lost from the monomer (peak 1) and dimer (peak 2) peaks appears as higher molecular weight products (peaks 3 and 4). Overall, the intensity of the peaks corresponding to oligomeric products increased in samples that initially contained higher protein concentrations. Figure 6B shows the results of equivalent experiments conducted with some of the Y → F mutants. Results obtained for the WT_{rec} protein are presented in the same plot for comparison. The oligomerization yields were calculated from the gel-filtration elution profiles and estimated by comparing the area of earlier eluting peaks (high molecular mass) with that of the peak area obtained for the monomeric protein before the addition of H_2O_2. The results show that oligomerization of both the Y146F mutant and the WT_{rec} protein is enhanced by high protein concentrations (Figure 6B). Surprisingly, incubation of the Y151F mutant at higher Mb concentrations also resulted in a modest but significant increase in the amount of cross-linked products even though no oligomeric species are observed at low protein concentrations. In contrast, the two proteins containing the Y103F mutation showed no dependence of the oligomerization yields on Mb concentration. With respect to the native protein, these two proteins showed approximately 40% decreases in the amount of cross-linked products formed at the highest concentrations of Mb. Moreover, the elution profiles of the two mutant proteins showed little evidence for tetramer or other multimer formation under these experimental conditions (not shown). Taken together, these results indicated that (i) at the lowest concentration range of Mb used in this study (40 μM metMb), Tyr151/ Tyr151 bonds dominate and (ii) at the highest concentrations of Mb (1280 μM metMb), a significant fraction of the cross-links are due to Tyr103/Tyr151 and/or Tyr103/Tyr103 cross-links.

Because of the high molar absorption of the SwMb Soret band ($\epsilon_{metMb,409}$ = 157 mM^{-1} cm^{-1}) (*20*), the kinetic experiments on autoreduction of the ferryl derivative were conducted with low protein concentrations (Figures 2 and 3). A large excess of H_2O_2 was used in all the experiments to ensure a rapid conversion of the metMb to the ferrylform. After 10 s, the excess of H_2O_2 was removed by the addition of catalase. The resulting solutions were analyzed by FPLC to estimate the yields of cross-linked proteins. The results in Table 3 indicate that up to ~40% of the monomeric enzyme is converted to dimeric products by this treatment. A modest amount of trimeric products was also detected in the incubations, but the protein showed no evidence of tetramer or other multimer formation under these experimental conditions. As observed in Table 2 for larger concentrations of the protein, removal of Tyr103 or Tyr146 does not interfere with oligomerization of the protein, and neither the Y151F nor the triple tyrosine mutant gave detectable cross-linked products.

Table 3: Relative Amount of Cross-Linked Products Formed under the Conditions Used for the Autoreduction Rate Measurements[a]

	% total Mb chain[b]		
	dimer	trimer	oligomer
WT_{rec}	43.5 ± 0.3	4.9 ± 0.3	nd[c]
Y146F	40.6 ± 0.3	5.9 ± 0.3	nd[c]
Y151F	nd[c]	nd[c]	nd[c]
K102Q/Y103F	41.2 ± 0.3	3.6 ± 0.3	nd[c]
K102Q/Y103F/Y146F	28.7 ± 0.4	2.8 ± 0.4	nd[c]
K102Q/Y103F/Y146F/Y151F	nd[c]	nd[c]	nd[c]

[a] Experimental conditions: SwMb (6.4 μM) in 50 mM potassium phosphate buffer, pH 6.8, at 25 °C. The reaction was initiated by the addition of H_2O_2 at a final concentration of 600 μM. After a 10 s incubation, the excess of H_2O_2 was removed by addition of catalase (26 units). The resulting solutions were incubated at 25 °C for 2 h and allowed to stand at 4 °C until subjected to FPLC as described under Experimental Procedures. [b] The relative amount of cross-linked products formed were calculated by deconvolution of the FPLC traces at 280 nm as described under Experimental Procedures. The number of Gaussian peaks contained in each chromatograph was fixed to three. [c] Not detectable.

Dependence of the Autoreduction Rate on Oligomerization State. A closer look at the kinetic traces obtained with the recombinant myoglobins show that the rapid phase of auto-

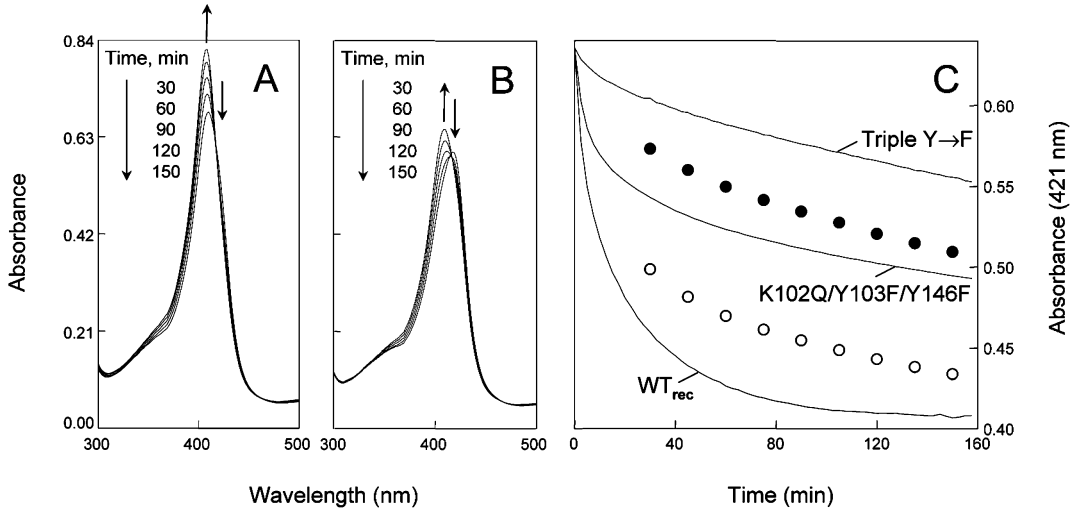

FIGURE 7: Dependence of the autoreduction rate on oligomerization state. (A) Spectral changes during the autoreduction of the dimeric form of H_2O_2-treated K102Q/Y103F/Y146F mutant. (B) Spectral changes during the autoreduction of the monomeric form of H_2O_2-treated K102Q/Y103F/Y146F mutant. (C) Time course of the autoreduction reaction at 421 nm (absorption maximum of the ferryl form). ●, monomer of the K102Q/Y103F/Y146F mutant; ○, dimer of the K102Q/Y103F/Y146F mutant; solid lines, preparations that have not been chromatographed. Experimental conditions: K102Q/Y103F/Y146F mutant (190 μM) in 50 mM potassium phosphate buffer, pH 6.8, at 25 °C. The reaction was initiated by the addition of H_2O_2 at final concentration of 600 μM. After 10 s incubation, the excess of H_2O_2 was removed by addition of catalase (26 units), and the resulting mixture was subjected to FPLC. The fractions corresponding to monomer and dimer forms of the K102Q/Y103F/Y146F mutant were pooled in two lots. The two lots were diluted to a final concentration of 6.4 μM in heme, and scans were taken at the time intervals indicated. The spectral changes were measured with an ordinary dual beam spectrophotometer.

reduction is largely associated with the presence of Tyr151, suggesting that either Tyr151 itself or a dimer of it is the primary source of rapid reducing equivalents in the enzyme. To discriminate between the two possibilities, we have performed additional experiments using the double Tyr → Phe mutant K102Q/Y103F/Y146F. This mutant retains Tyr151 and is thus still capable of dimerizing upon incubation with H_2O_2.

H_2O_2 was added to the double Tyr → Phe mutant, and the resulting dimer was rapidly separated from the monomer by gel-filtration chromatography (not shown). A large proportion of these two proteins remained in the ferryl state after the separation. Figure 7A shows the absorption changes in the Soret and visible regions during autoreduction of the dimer of the double Tyr → Phe mutant. Figure 7B shows the equivalent experiment conducted with the monomer of the double Tyr → Phe mutant. The time course of the autoreduction at 421 nm of pooled fractions of the monomer and the dimer is presented in Figure 7C. The time courses of the autoreduction of a preparation of the double Tyr → Phe mutant that had not been chromatographed and of the wild-type and the triple Tyr → Phe mutant are presented in the same plot for comparison. The first measurements were carried out 30 min after addition of H_2O_2 to the reaction mixture (e.g., a few minutes after elution of the chromatographic peak from the column).

The change in absorbance at 421 nm of the dimer of the double Tyr → Phe mutant indicates that approximately 50% of the ferryl form is converted to the ferric form during the first 30 min (Figure 7C). This is twice as much as the change observed for the preparation of the double Tyr → Phe mutant prior to chromatographic separation of the monomeric and oligomeric proteins. After this initial rapid decrease, the absorbance continues to decrease slowly. The results are consistent with the dimer of Tyr151 being a major source of reducing equivalents within the enzyme.

The equivalent experiment conducted with the monomer of the double Tyr → Phe mutant showed that the rapid phase of spontaneous ferryl reduction is considerably reduced; the change in intensity after 30 min is this time lower than the change observed for the preparation of the double mutant that has not been chromatographed. Nevertheless, the recovered Y151F monomer undergoes autoreduction more rapidly that the triple tyrosine mutant, which indicates that Tyr151 alone is able to donate electrons for reduction of the ferryl species, albeit less effectively than the Tyr151−Tyr151 substructure. It is also clear from Figure 3B that Tyr103 is able to reduce the ferryl species, as the Y151F mutant undergoes autoreduction considerably faster than the triple tyrosine mutant.

DISCUSSION

The reaction of SwMb with H_2O_2 yields a ferryl species and a transient, protein-associated radical that is dissipated by incompletely understood mechanisms. Furthermore, over time, the SwMb ferryl species undergoes an autoreduction that regenerates the ferric enzyme. This experimental system has been employed here to investigate the roles of the individual oxidizable residues in the protein in the autoreduction process, as it provides a structurally well-defined system in which to evaluate the factors that control electron transfer from amino acid residues to a fixed electron-deficient center. This was done by removing individual amino acids and determining the effects of their absence or presence on the rate of reduction of the ferryl intermediate to the ferric state. The amino acids of particular interest were the three tyrosines (Tyr103, Tyr146, and Tyr151) and the two tryptophans (Trp7 and Trp14), as these are the residues that might be expected to act as electron donors and for which experimental evidence is available supporting that they are actually oxidized in the reaction of SwMb with H_2O_2.

The rates of formation of the ferryl species in the reactions of H_2O_2 with recombinant SwMb and its W7F, W14F,

Y146F, Y151F, K102Q/Y103F, and K102Q/Y103F/Y146F/Y151F triple tyrosine mutant shows that the tyrosine mutations have a negligible effect on ferryl formation (Table 1). Not only is the rate of the WT_{rec} very similar to that of the native protein, but also the rates for all the mutants are also very similar. The rate for the W7F mutant, which shows the largest difference, is only 20% lower than that for the WT_{nat} enzyme. The ferryl species is thus formed at comparable rates with all the proteins that were investigated, making it possible to use a single experimental protocol for the ferryl autoreduction measurements. In this protocol, the proteins are incubated with excess H_2O_2 for 10 s, after which the excess H_2O_2 is quenched by adding catalase. The disappearance of the ferryl species can then be monitored without having to worry about reoxidation of the ferric enzyme by excess H_2O_2.

Using the previous protocol, we have found that the autoreduction is a biphasic, or possibly higher order, process. For the WT_{rec} enzyme, the fast phase corresponds to $k_{1obs} = 5.24 \times 10^{-3}$ s^{-1} ($t_{1/2} = 2.2$ min) and the slow phase to $k_{2obs} = 5.73 \times 10^{-4}$ s^{-1} ($t_{1/2} = 20.2$ min). The fast phase accounts for reduction of 34% of the initial ferryl species. As shown in Figure 3B, the rapid phase of ferryl reduction is suppressed in the absence of all three tyrosine residues, although a slow reduction is observed even in their absence. Elimination of Tyr146 alone has no effect on autoreduction, so this residue does not detectably contribute to this process. However, in the absence of either Tyr151 or Tyr103, the rapid phase of ferryl reduction is decreased to approximately half of its value in the WT_{rec} protein, so both of these tyrosines contribute to ferryl autoreduction.

Electron transfer from either Tyr151 or Tyr103 during the initial reaction with H_2O_2 results in formation of the corresponding tyrosine radical, and combination of two such radicals leads to the formation of Tyr−Tyr linked homodimers (*8*, *9*, *12*). As the dityrosine links could make a unique contribution to the ferryl autoreduction, we have analyzed the extent and type of protein oligomerization. The same distribution of oligomeric products is obtained with the WT_{nat} and WT_{rec} proteins (Figure 5 and Table 2). Indeed, similar product distributions are found for the Trp7, Trp14, Tyr103, and Tyr146 single mutants. However, the Y151F mutation, as reported (*8*), suppresses protein oligomerization at low protein concentrations (Figure 5). Analysis of the protein-dependence of dimer formation indicates that at low SwMb protein concentrations, the dominant cross-link is Tyr151−Tyr151, whereas at higher protein concentrations there is also significant formation of Try151−Tyr103 and possibly Tyr103−Tyr103 cross-links (Figure 6). Under the conditions used for the autoreduction rate measurements, the primary product is a Tyr151−Tyr151 dimer.

It is also known that Tyr103 cross-links to the heme group under some conditions, and this could be envisioned as also playing a role in altering ferryl group autoreduction (*22*). However, as previously shown (*10*), formation of the Tyr103−heme link is pH dependent and is minimal at pH 6.8. This process is therefore unlikely to play a significant role in the electron transfer observed here.

Analysis of the autoreduction data for the mutant proteins indicates that the rapid autoreduction phase is largely, but not entirely, dependent on the presence of Tyr151. Incubation of the double Tyr → Phe mutant that only retains Tyr151 with H_2O_2, followed by chromatographic separation of the resulting monomeric and dimeric protein fractions, has allowed us to examine the dependence of the autoreduction rate on the oligomerization state (Figure 7). Interestingly, the dimer is seen to undergo fast phase autoreduction more rapidly than the recovered monomer, and the monomer in turn autoreduces more rapidly than the triple tyrosine mutant. If the contributions to the fast phase of the monomer and dimer are compared to the overall rate of autoreduction for the mixture before chromatographic separation, it appears that the dimer accounts for approximately two-thirds of the fast phase and the monomer for one-third. The oligomerization yields in Table 2 indicate that approximately two-thirds of the K102Q/Y103F/Y146F protein is monomeric and one-third is oligomeric. The smaller fraction of this double mutant in the dimeric state thus accounts for the major fraction of the observed fast autoreduction and the somewhat larger monomeric fraction for the remaining. In the presence of Tyr103, however, there is also a contribution by Tyr103, as shown in Figure 3B.

Comparison of the redox potentials of tyrosine and tryptophan residues readily rationalizes the observation that the tyrosines but not tryptophans participate in autoreduction. Thus, the reduction potentials of tyrosine residues determined by pulse radiolysis and cyclic voltammetry fall in the range of 0.85−0.94 V and those of tryptophan residues in the range of 1.03−1.08 V (*23*−*28*). These values are to be compared with a value of approximately 0.9 V for ferryl Mb (*29*). Thus, the tyrosine potentials favor electron transfer to the ferryl species to a much greater extent than those of the tryptophans. It is also possible to discriminate among the tyrosine residues. Calculations of the solvent exposure of the three tyrosines suggests the values of 78.15, 35.12, and 2.44 Å^2 for Tyr151, Tyr103, and Tyr146, respectively, which roughly parallels the pK_a values determined for these three residues: Tyr151, pK_a = 10.3; Tyr103, pK_a = 11.8−12.0; and Tyr146, pK_a = 12.8−12.9 (*30*). On the other hand, the distances of the closest ring carbon of Tyr103, Tyr146, and Tyr151 from the iron atom in the SwMb crystal structure are 9.66 (*meta* ring carbon), 9.49 (oxygen-substituted ring carbon), and 11.65 Å (*ortho* ring carbon), respectively. In the case of Tyr146, the phenol oxygen actually points toward the iron and, at a distance of 8.17 Å, is the closest atom to it. The phenol oxygen in the other two tyrosines is further away from the iron than the closest ring carbon indicated previously. The edges of the porphyrin ring—either the *meso* bridges or pyrrole rings—could also function as conduits for the electron transfer. The distances from the tyrosine residues to the heme edge must therefore also be taken into consideration. The distance of closest approach of a porphyrin ring carbon to a carbon of Tyr103, Tyr146, and Tyr151 is 3.54 (*meta* carbon), 8.65 (oxygen-substituted carbon), and 10.10 Å (*ortho* ring carbon), respectively. For Tyr146 and Tyr151, the point of closest approach is actually the phenol oxygen, which is located at a distance of 7.31 and 9.06 Å from the heme group, respectively. Thus, the SwMb crystal structure indicates that Tyr103 is closest to the heme, and Tyr151 is the most distant. These results suggest that the reduction potentials of the tyrosines, which roughly correlate with solvent exposure and pK_a, are key determinants of the ability to donate electrons regardless of the distance from the ferryl iron or heme edge. Thus, Tyr146, the least exposed tyrosine with the highest pK_a value, does

not contribute to autoreduction even though it is closer to the ferryl iron than either Tyr103 or Tyr151 and closer to a ring edge than Tyr151.

Reeder and Wilson have reported that ferryl autoreduction is pH dependent and have attributed this to protonation of a group near the heme, possibly the ferryl species itself (*31*). Changes in the pK_a of this site caused by the Tyr → Phe mutations could conceivably contribute to the differences in autoreduction rates observed here. This contribution cannot be ruled out without a full study of the pH dependence of the process but is unlikely to be major because the electron-transfer rates correlate well with solvent exposure and tyrosine pK_a.

The finding that the Tyr151−Tyr151 dityrosine link in the Y103F/Y146F dimer is a major contributor to the fast autoreduction phase is consistent with an important role in the reduction potential of the residue in determining its participation in the autoreduction. We have demonstrated in previous work that both dityrosine and isodityrosine are found as the cross-linking group in oligomeric SwMb (*10*). Although we have been unable to find the reduction potential of dityrosine or isodityrosine in the literature, the pK_a values of dityrosine and isodityrosine are 6.7 and 9.8, respectively (*32*). At pH 7.0, more than half of the dityrosine will be in the monodeprotonated state, and even the isodityrosine will be ionized to a greater extent than any of the three tyrosines in the native protein. Furthermore, the reduction potential of dityrosine is expected to be lower than that of tyrosine due to intramolecular hydrogen bonding between the vicinal phenolic hydroxyl groups and enhanced conjugative stabilization of the corresponding radical. Thus, even though it is located at a greater distance than Tyr103 or Tyr146, and at the same distance as Tyr151 in the monomeric protein, the Tyr151−Tyr151 cross-linking moiety contributes disproportionately to the fast phase of ferryl autoreduction. It is clear from these results that the redox potential, which is related to the pK_a of the phenol, is more critical for electron donation to the ferryl group than the distance that separates the two groups.

ACKNOWLEDGMENT

We thank Angela Wilks and Richard Tschirret-Guth for the original SwMb mutant constructs.

REFERENCES

1. Keilin, D., and Hartree, E. F. (1950) Reaction of methæmoglobin with hydrogen peroxide, *Nature 166*, 513−514.
2. King, N. K., and Looney, F. D., and Winfield, M. E. (1967) Amino acid free radicals in oxidized metmyoglobin, *Biochim. Biophys. Acta 133*, 65−82.
3. Yonetani, T., and Schleyer, H. (1967) Electromagnetic properties of hemoproteins. II. The effect of physical states on electron paramagnetic resonance parameters of hemoproteins, *J. Biol. Chem. 242*, 1974−1979.
4. Miki, H., Harada, K., Yamazaki, I., Tamura, M., and Watanabe, H. (1989) Electron spin resonance spectrum of Tyr-151 free radical formed in reactions of sperm whale metmyoglobin with ethyl hydroperoxide and potassium irridate, *Arch. Biochem. Biophys. 275*, 354−362.
5. Gunther, M. R., Tschirret-Guth, R. A., Witkowska, H. E., Fann, Y. C., Barr, D. P., Ortiz de Montellano, P. R., and Mason, R. P. (1998) Site-specific spin trapping of tyrosine radicals in the oxidation of metmyoglobin by hydrogen peroxide, *Biochem. J. 330*, 1293−1299.
6. Davies, M. J. (1990) Detection of myoglobin-derived radicals on reaction of metmyoglobin with hydrogen peroxide and other peroxidic compounds, *Free Rad. Res. Commun. 10*, 361−370.
7. Xu, Y., Asghar, A., Gray, J. I., Pearson, A. M., Haug, A., and Grulke, E. A. (1990) ESR spin-trapping studies of free-radicals generated by hydrogen-peroxide activation of metmyoglobin, *J. Agric. Food Chem. 38*, 1494−1497.
8. Wilks, A., and Ortiz de Montellano, P. R. (1992) Intramolecular translocation of the protein radical formed in the reaction of recombinant sperm whale myoglobin with H_2O_2, *J. Biol. Chem. 267*, 8827−8833.
9. Tschirret-Guth, R. A., and Ortiz de Montellano, P. R. (1996) Protein radicals in myoglobin dimerization and myoglobin-catalyzed styrene epoxidation, *Arch. Biochem. Biophys. 335*, 93−101.
10. Lardinois, O. M., and Ortiz de Montellano, P. R. (2003) Intra- and intermolecular transfers of protein radicals in the reactions of sperm whale myoglobin with hydrogen peroxide, *J. Biol. Chem. 278*, 36214−36226.
11. Dayhoff, M. O., Hunt, L. T., McLaughline, P. J., and Jones, D. D. (1976) *Atlas of Protein Sequence and Structure* (Dayhoff, M. O., Ed.) Vol. 5, Suppl. 2, p 208, National Biomedical Research Foundation, MD.
12. Tew, D., and Ortiz de Montellano, P. R. (1988) The myoglobin protein radical. Coupling of Tyr-103 to Tyr-151 in the H_2O_2-mediated cross-linking of sperm whale myoglobin, *J. Biol. Chem. 263*, 17880−17886.
13. DeGray, J. A., Gunther, M. R., Tschirret-Guth, R., Ortiz de Montellano, P. R., and Mason, R. P. (1997) Peroxidation of a specific tryptophan of metmyoglobin by hydrogen peroxide, *J. Biol. Chem. 272*, 2359−2362.
14. Gunther, M. R., Tschirret-Guth, R. A., Lardinois, O. M., and Ortiz de Montellano, P. R. (2003) Tryptophan-14 is the preferred site of DBNBS spin trapping in the self-peroxidation reaction of sperm whale metmyoglobin with a single equivalent of hydrogen peroxide, *Chem. Res. Toxicol. 16*, 652−660.
15. Harris, M. N., Burchiel, S. W., Winyard, P. G., Engen, J. R., Mobarak, C. D., and Timmins, G. S. (2002) Determining the site of spin trapping of the equine myoglobin radical by combined use of EPR, electrophoretic purification, and mass spectrometry, *Chem. Res. Toxicol. 15*, 1589−1594.
16. Fenwick, C. W., and English, A. M. (1996). Trapping and LC-MS identification of protein radicals formed in the horse heart metmyoglobin-H_2O_2 reaction, *J. Am. Chem. Soc. 118*, 12236−12237.
17. King, N. K., and Winfield, M. E. (1963) The mechanism of metmyoglobin oxidation, *J. Biol. Chem. 238*, 1520−1528.
18. Fry, S. C. (1984) Isodityrosine, a diphenyl ether cross-link in plant-cell wall glycoprotein—identification, assay, and chemical synthesis, *Methods Enzymol. 107*, 388−397.
19. Lardinois, O. M., and Ortiz de Montellano, P. R. (2001) H_2O_2-mediated cross-linking between lactoperoxidase and myoglobin: elucidation of protein−protein radical transfer reactions, *J. Biol. Chem. 276*, 23186−23191.
20. Antonini, E., and Brunori, M. (1971) The derivatives of ferric hemoglobin and myoglobin, in *Hemoglobin and Myoglobin in Their Reactions with Ligands* (Neuberger, A., and Tatum, E. L., Eds.) Ch. 3, p 44, North-Holland Publishing Company, London.
21. Witting, P. K., Mauk, A. G., and Lay, P. A. (2002) Role of tyrosine-103 in myoglobin peroxidase activity: kinetic and steady-state studies on the reaction of wild-type and variant recombinant human myoglobins with H_2O_2, *Biochemistry 41*, 11495−11503.
22. Catalano, C. E., Choe, Y. S., and Ortiz de Montellano, P. R. (1989) Reactions of the protein radical in peroxide-treated myoglobin. Formation of a heme−protein cross-link, *J. Biol. Chem. 264*, 10534−10541.
23. DeFelippis, M. R., Murthy, C. P., Faraggi, M., and Klapper, M. H. (1989) Pulse radiolytic measurement of redox potentials: the tyrosine and tryptophan radicals, *Biochemistry 28*, 4847−4853.
24. Jovanovic, S. V., Steenken, S., and Simic, M. G. (1991) Kinetics and energetics of one-electron-transfer reactions involving tryptophan neutral and cation radicals, *J. Phys. Chem. 95*, 684−687.
25. Merenyi, G., Lind, J., and Shen, X. H. (1988) Electron-transfer from indoles, phenol, and sulfite (SO_3^{2-} to chlorine dioxide (ClO_2)), *J. Phys. Chem. 92*, 134−137.
26. Tommos, C., Skalicky, J. J., Pilloud, D. L., Wand, A. J., and Dutton, P. L. (1999) *De novo* proteins as models of radical enzymes, *Biochemistry 38*, 9495−9507.

27. Jovanovic, S. V., Harriman, A., and Simic, M. G. (1986) Electron-transfer reactions of tryptophan and tyrosine derivatives, *J. Phys. Chem. 90*, 1935−1939.
28. Lind, J., Shen, X., Eriksen, T. E. et al. (1990) The one-electron reduction potential of 4-substituted phenoxyl radicals in water, *J. Am. Chem. Soc. 112*, 479−482.
29. He, B., Sinclair, R., Copeland, B. R., Makino, R., Powers, L. S., and Yamazaki, I. (1996) The structure−function relationship and reduction potentials of high oxidation states of myoglobin and peroxidase, *Biochemistry 35*, 2413−2420.
30. Uyeda, M., and Peisach, J. (1981) Ultraviolet difference spectroscopy of myoglobin: assignment of p*K* values of tyrosyl phenolic groups and the stability of the ferryl derivatives, *Biochemistry 20*, 2028−2035.
31. Reeder, B. J., and Wilson, M. T. (2001) The effects of pH on the mechanism of hydrogen peroxide and lipid hydroperoxide consumption by myoglobin: a role for the protonated ferryl species, *Free Radical Biol. Med. 30*, 1311−1318.
32. Fry, S. C. (1992) Isodityrosine, a new cross-linking amino acid from plant cell-wall glycoprotein, *Biochem. J. 204*, 449−455.

BI036241B